

NA

NASA CR-165563

(NASA-CR-165563) FATIGUE LIFE PREDICTION IN  
BENDING FROM AXIAL FATIGUE INFORMATION (Case  
Western Reserve Univ.) 38 p HC A03/MF A01  
CSCI 20K

N82-20564

Unclas  
G3/39 09385

FATIGUE LIFE PREDICTION IN BENDING  
FROM AXIAL FATIGUE INFORMATION

S. S. Manson  
Professor, Mechanical and Aerospace Engineering

and

U. Muralidharan  
Research Assistant



Case Western Reserve University  
Cleveland, Ohio 44106

February 1982

NASA CR-165563

FATIGUE LIFE PREDICTION IN BENDING  
FROM AXIAL FATIGUE INFORMATION

S. S. Manson  
Professor, Mechanical and Aerospace Engineering

and

U. Muralidharan  
Research Assistant

Case Western Reserve University  
Cleveland, Ohio 44106

February 1982

## INTRODUCTION

It is common to express the bending fatigue life of a material in terms of the nominal elastic stress or strain calculated by assuming stress is proportional to strain. Yet, in the low-cycle fatigue range, and in fact over a wide range of life of engineering interest, plastic flow is involved, and stress is not proportional to strain. Thus considerable discrepancy exists between bending fatigue and axial fatigue when the latter involves expression in terms of true stresses and strains. While several factors contribute to this discrepancy, as discussed in Ref. 1, among them the presence of strain gradient, a volumetric effect, cyclic strain hardening and softening effects, and crack propagation differences after the surface stress has been initiated, the major effect is due to the fact that the nominal stress and strains on a specimen in bending differ considerably from the true values due to plastic deformation.

In Ref. 1, it was demonstrated that flexural fatigue is considerably different from axial fatigue, but that the two could be brought into coincidence when based on true surface stresses. Fig. 1 shows some of the results of the reference. The solid curve and circular data points show the axial fatigue characteristic of 4130 steel. In this case the stresses are true values because in axial loading it is simple to determine the stress from a knowledge of load and cross-sectional area. The dashed curve and square data points refer to the beam bending

characteristics. Here the stress is calculated from the conventional  $S = \frac{Mc}{I}$  assumptions, so that the stresses are the fictitious values determined on the basis that no plastic flow occurs. It is seen that for this material the nominal bending stress can be 50% higher at the 100 cycle life level, and that significant difference persists between the two curves until well above  $10^5$  cycles to failure. Obviously, then, it is important to reconcile the differences over a wide range of life levels of practical engineering interest. It was also demonstrated in Ref. 1, that if the true stress is calculated in the case of the bending specimen the life comparison with the axially loaded comparison is much more favorable. But, because of the difficulty of performing the integrations involved in the bending case no closed-form solution was presented. Each material and geometry had to be treated numerically.

It is the purpose of this report to extend the work of Ref. 1 and to obtain closed-form generalized relationships. The approach is first to study rectangular rather than circular sections. Not only are rectangular sections of great importance in engineering applications, but they result in relations that can be integrated in closed-form. The resulting form of the solutions then provides a model for use in the case of circular sections. By assuming an analogous model, involving several undetermined constants, and then determining the constants so as to fit a range of known solutions obtained by numerical integration, it has been possible to obtain very accurate, though not exact, closed-form solutions for the case of the circular section. The procedure and results will be described in this report.

In addition to the development of plasticity as a reason for difference between axial and bending fatigue, another factor relating to volume under stress also introduces differences in the lives of the two loading modes. In pure axial loading the entire cross section of the specimen is subjected to the loading stress, whereas in pure bending only the surface fibers are subjected to the maximum stress, while other regions of the cross section are subjected to lower stresses. The effect of this factor is expected to be important in the high cycle fatigue range, rather than the low cycle fatigue range which is of major interest in this report. However, this subject is also briefly discussed.

#### BASIC EQUATIONS USED FOR LIFE RELATIONSHIPS

##### The Conventional Life Relationship

The basic model for axial fatigue used in this report is shown in Fig. 2. Although the model was first proposed by Manson (Ref. 2) using a different notation, the notation used in Fig. 2 is the one that has been commonly adopted (Ref. 3). The strain amplitude,  $\frac{\Delta\epsilon}{2}$  is plotted on the vertical axis, and the number of reversals  $2N_f$  on the horizontal axis, using logarithmic scales on both axes. If a material is axially cycled at constant strain range about a zero mean value, or if the plastic strain range is maintained constant, it is generally found that in the early cycles the stress (or, equivalently, the elastic strain) may change considerably, but eventually a saturation value is

achieved. Usually this saturation value develops early and persists for the major part of the life of the specimen. Plots such as shown in Fig. 2, in which both the plastic strain amplitude, and the elastic strain amplitude, are plotted against reversals to failure result in straight lines PQ and LM, the equations of which are, respectively,

$$\frac{\Delta \epsilon_p}{2} = \epsilon_f' (2N_f)^c \quad (1)$$

$$\frac{\Delta \epsilon_e}{2} = \frac{\Delta \sigma}{2E} = \frac{\sigma_f'}{E} (2N_f)^b \quad (2)$$

where  $\Delta \epsilon_p$  is the plastic strainrange,  $\Delta \epsilon_e$  is the elastic strainrange, and  $\Delta \sigma$  the saturation stress range,  $\epsilon_f'$  and  $\frac{\sigma_f'}{E}$  are the intercepts at  $2N_f = 1$  of the plastic and elastic lines,  $E$  is the elastic modulus, and  $c$  and  $b$  are the slopes of the two lines as shown in Fig. 2.

The equation for the total strain amplitude, which is the sum of the plastic and elastic components, is thus

$$\frac{\Delta \epsilon}{2} = \epsilon_f' (2N_f)^c + \frac{\sigma_f'}{E} (2N_f)^b \quad (3)$$

In Ref. 4 we introduced the term "transition life" to designate the life at the intersection point T of the elastic and plastic lines. In Fig. 2 this life is denoted  $N_T$  and the number of reversals is  $2N_T$ . Correspondingly, the strainrange at this point is  $\Delta \epsilon_T$  and the strain amplitude is  $\Delta \epsilon_T/2$ . By equating the strains in Eqs. (1) and (2) the values of  $N_T$  and  $\Delta \epsilon_T$  can easily be determined.

$$N_T = \frac{1}{2} \left( \frac{E \epsilon'_f}{\sigma'_f} \right)^{\frac{1}{b-c}} \quad (4)$$

$$\begin{aligned} \Delta \epsilon_T &= 2 \left( \epsilon'_f \right)^{\frac{b}{b-c}} \left( \frac{\sigma'_f}{E} \right)^{\frac{c}{c-b}} \\ &= 2 \left( \epsilon'_f \right)^{\frac{1}{1-n}} \left( \frac{\sigma'_f}{E} \right)^{\frac{n}{n-1}} \end{aligned} \quad (5)$$

where  $n = \frac{c}{b}$ . It may be noted that  $n$  is the reciprocal of the strain hardening exponent  $m'$  in the relation  $\Delta \sigma = \text{Constant } (\Delta \epsilon_p)^{m'}$ . From Eqs. (4) and (5) it can readily be shown that the basic life model Eq. (3) can be rewritten [5]

$$\frac{\Delta \epsilon}{\Delta \epsilon_T} = \left( \frac{N_f}{N_T} \right)^c + \left( \frac{N_f}{N_T} \right)^b \quad (6)$$

#### The Inverted Life Relation

For convenience in some of the numerical integration analyses we have also used an alternative form of the life relation discussed in Ref. 6. Basically, life is expressed directly in terms of strain, instead of using Eq. (6) which expresses strain in terms of life

$$\frac{N_f}{N_T} = \left[ R_{\epsilon}^{\frac{z}{c}} + R_{\epsilon}^{\frac{z}{b}} \right]^{\frac{1}{z}} \quad (7)$$

where

$$z = \exp \left[ P \ln^2 R_\epsilon + Q \ln R_\epsilon + \ln \left( -0.889c \left( \frac{c}{b} \right)^{-0.36} \right) \right] \quad (8)$$

$$P = -0.001277 \left( \frac{c}{b} \right)^2 + 0.03893 \left( \frac{c}{b} \right) - 0.0927 \quad (9)$$

$$Q = +0.004176 \left( \frac{c}{b} \right)^2 - 0.135 \left( \frac{c}{b} \right) + 0.2309 \quad (10)$$

$$R_\epsilon = \frac{\Delta \epsilon}{\Delta \epsilon_T} = \text{ratio of strain required to produce life } N_f \text{ to} \\ \text{the transition strain} \quad (11)$$

For any material of known  $b$ ,  $c$ ,  $N_T$  and  $\Delta \epsilon_T$ , all the constants involved in the equations are readily calculated, the life  $N_f$  is expressed directly in terms of those constants and strainrange.

Similarly, stress range  $\Delta \sigma$  can be written directly in terms of applied strainrange  $\Delta \epsilon$

$$\Delta \sigma = E \Delta \epsilon_T \left[ R_\epsilon^{z/b} + R_\epsilon^{z/c} \right]^{b/z} \quad (12)$$

The Universal Slopes Life Equation: In cases where material constants  $b$ ,  $c$ ,  $\epsilon'_f$  and  $\sigma'_f$  are not accurately known from experiment, it may be desired to estimate the life relation on the basis of commonly available material properties. In Ref. 1 it was demonstrated that as a first approximation  $c$  could be taken as a universal value of -0.6,  $b$  as a universal value of -0.12, and that  $\epsilon'_f$  could be estimated from the ductility, while  $\sigma'_f$  was best estimated from ultimate tensile strength. The resulting "universal-slopes" equation, as expressed in Ref. (1), is\*,

$$\Delta \epsilon = D^{0.6} N_f^{-0.6} + \frac{3.5 \sigma_u}{E} N_f^{-0.12} \quad (13)$$

---

\* While this equation is generally credited only to Manson because it first appeared in Ref. 1, the equal contribution of M. H. Hirschberg in its development is acknowledged.



where

$D$  = ductility =  $-\ln(1-RA)$  wherein  $RA$  is reduction of area in tensile test

$\sigma_u$  = ultimate tensile strength, and  $E$  is elastic modulus in consistent units.

Expressed with the SAE notation of Eq. (3), the equation becomes

$$\frac{\Delta \epsilon}{2} = 0.7578D^{0.6}(2N_f)^{-0.6} + 1.902 \frac{\sigma_u}{E} (2N_f)^{-0.12} \quad (14)$$

$$\text{That is, } \epsilon'_f = 0.7578D^{0.6} \text{ and } \sigma'_f = 1.902\sigma_u \quad (15)$$

Also, using Eqs. (4) and (5),

$$\Delta \epsilon_T = 4.789 \left(\frac{\sigma_u}{E}\right)^{1.25} D^{-.15} \quad (16)$$

$$N_T = .0735 \left(\frac{\sigma_u}{E}\right)^{-2.083} D^{1.25} \quad (17)$$

so that Eq. (6) becomes

$$\frac{\Delta \epsilon}{\Delta \epsilon_T} = \left[ \frac{N_f}{N_T} \right]^{-0.6} + \left[ \frac{N_f}{N_T} \right]^{-0.12} \quad (18)$$

where  $\Delta \epsilon_T$  and  $N_T$  are given by Eqs. (16) and (17), respectively.

Similarly, substituting  $c = -0.6$ ,  $b = -0.12$  into Eqs. (9) and (10), we obtain  $P = .07$ ,  $Q = -.3397$

$$z = \exp[.07 \ln^2 R_E - .3397 \ln R_E - 1.208]$$

$$R_E = \frac{\Delta \epsilon}{\Delta \epsilon_T}$$

$$N_f = N_T [R_E^{z/c} + R_E^{z/b}]^{1/2} \quad (19)$$

where  $\Delta \epsilon_T$ ,  $N_T$  are given by Eqs. (16) and (17), respectively.

### FLXURAL BENDING OF RECTANGULAR CROSS-SECTIONS

We first treat the bending of rectangular cross-sections because the resulting equations can be integrated in closed form. As discussed in Ref. 1, it is more convenient to solve this type of problem in an inverse fashion compared to conventional treatment. Rather than starting with a known bending moment, and determining the resulting surface strain--which would involve solution of non-linear equations--it has been found better to select a surface strain and calculate the bending moment required to produce this strain. From the selected surface strain we establish the fatigue life, and from the required bending moment the nominal elastic stress. Thus we can establish the relation between nominal elastic stress and fatigue life.

Fig. 3 shows the notation used in the analysis. We assume a surface strain  $\epsilon_s$  corresponding to a life  $N_s$  when the full bending moment  $M$  is applied. Since in bending it is common to assume that plane sections remain plane, strain varies linearly across the thickness, so that the strain  $\epsilon_y$  at a distance  $y$  from the neutral axis (center of bar) is

$$\epsilon_y = \frac{y}{h} \epsilon_s \quad (20)$$

Substituting for  $\epsilon_s$  in terms of life  $N_s$  associated with the surface strain, from Eq. (6)\*

$$\epsilon_y = \frac{y\epsilon_T}{h} \left[ \left( \frac{N_s}{N_T} \right)^b + \left( \frac{N_s}{N_T} \right)^c \right] \quad (21)$$

\*Because of the symmetry of loading for this case of completely reversed bending, we omit the  $\Delta$ 's, and consider only surface strains at the maximum loading condition.

Now if  $N_y$  is the life associated with the strain at  $y$ , then by Eq. (6)

$$\frac{\epsilon_y}{\epsilon_T} = \left( \frac{N_y}{N_T} \right)^b + \left( \frac{N_y}{N_T} \right)^c \quad (22)$$

and the stress associated with the strain  $\epsilon_y$  is, as derived from Eqs. (2), (4) and (5),

$$\sigma_y = E \epsilon_T \left( \frac{N_y}{N_T} \right)^b \quad (23)$$

The increment of bending moment contributed by a strip  $w dy$  at the distance  $y$  from the neutral axis becomes

$$dM = y \cdot \sigma_y w dy = E \epsilon_T \left( \frac{N_y}{N_T} \right)^b \cdot wy dy \quad (24)$$

and the total bending moment, taking into account the symmetrical contribution to bending moment of the section below the neutral axis is

$$M = \int dM = 2Ew\epsilon_T \int_0^{y=h} \left( \frac{N_y}{N_T} \right)^b y dy \quad (25)$$

Here  $N_y$  is a function of  $y$  according to Eqs. (21) and (22). In order to carry out the integration it is best to establish  $dy$  in terms of  $\frac{N_y}{N_T}$ , rather than expressing  $\frac{N_y}{N_T}$  in terms of  $y$ , which would result in a more difficult integration. Thus from Eq. (21) and (22),

$$y = h \frac{\left( \frac{N_y}{N_T} \right)^b + \left( \frac{N_y}{N_T} \right)^c}{\left( \frac{N_S}{N_T} \right)^b + \left( \frac{N_S}{N_T} \right)^c} \quad (26)$$

and

$$dy = \frac{h}{\left(\frac{N_S}{N_T}\right)^b + \left(\frac{N_S}{N_T}\right)^c} \left[ b \left(\frac{N_Y}{N_T}\right)^{b-1} + c \left(\frac{N_Y}{N_T}\right)^{c-1} \right] d \left[ \frac{N_Y}{N_T} \right] \quad (27)$$

From Eq. (25), therefore,

$$M = \frac{2Ew h^2 \epsilon_T}{\left[ \left(\frac{N_S}{N_T}\right)^b + \left(\frac{N_S}{N_T}\right)^c \right]^2} \int_0^{\frac{N_S}{N_T}} \left[ b \left(\frac{N_Y}{N_T}\right)^{2b-1} + c \left(\frac{N_Y}{N_T}\right)^{b+c-1} \right] \left[ \left(\frac{N_Y}{N_T}\right)^b + \left(\frac{N_Y}{N_T}\right)^c \right] d \left(\frac{N_Y}{N_T}\right) \quad (28)$$

$$= \frac{2Ew h^2 \epsilon_T}{\left[ \left(\frac{N_S}{N_T}\right)^b + \left(\frac{N_S}{N_T}\right)^c \right]^2} \int_0^{\frac{N_S}{N_T}} \left[ b \left(\frac{N_Y}{N_T}\right)^{3b-1} + b \left(\frac{N_Y}{N_T}\right)^{2b+c-1} + c \left(\frac{N_Y}{N_T}\right)^{2b+c-1} + c \left(\frac{N_Y}{N_T}\right)^{b+2c-1} \right] d \left(\frac{N_Y}{N_T}\right) \quad (29)$$

$$= \frac{2Ew h^2 \epsilon_T}{\left[ \left(\frac{N_S}{N_T}\right)^b + \left(\frac{N_S}{N_T}\right)^c \right]^2} \left[ \frac{b}{3b} \left(\frac{N_Y}{N_T}\right)^{3b} + \frac{b+c}{2b+c} \left(\frac{N_Y}{N_T}\right)^{2b+c} + \frac{c}{b+2c} \left(\frac{N_Y}{N_T}\right)^{b+2c} \right] \Bigg|_0^{\frac{N_S}{N_T}} \quad (30)$$

In Eqs. (28), (29) and (30) the lower limit for  $\frac{N_Y}{N_T}$  is taken at  $h = 0$ , where the strain is zero, and therefore the life is infinite.

Since all the exponents of  $\frac{N_S}{N_T}$  in the integrated expression are negative, the value of all terms is zero at the lower limit, and M is evaluated as

$$M = 2Ew h^2 \epsilon_T \frac{\frac{1}{3} \left(\frac{N_S}{N_T}\right)^{3b} + \frac{b+c}{2b+c} \left(\frac{N_S}{N_T}\right)^{2b+c} + \frac{c}{b+2c} \left(\frac{N_S}{N_T}\right)^{b+2c}}{\left(\frac{N_S}{N_T}\right)^{2b} + 2 \left(\frac{N_S}{N_T}\right)^{b+c} + \left(\frac{N_S}{N_T}\right)^{2c}} \quad (31)$$

The nominal surface stress  $S_{\text{bending}}$  is  $\frac{Mh}{I} = \frac{12Mh}{w(2h)^3} = \frac{12M}{8wh^2}$  since the total height of the rectangle is  $2h$  and the moment of inertia of a rectangular section is  $\frac{1}{12}$  base  $\times$  (height)<sup>3</sup>. Thus, substituting for M from Eq. (31), and dividing both numerator and denominator by  $\left(\frac{N_S}{N_T}\right)^{2b}$ , the resulting equation for  $S_{\text{bending}}$  is obtained as follows:

$$S_{\text{bending}} = E\epsilon_T \left(\frac{N_S}{N_T}\right)^b \left[ \frac{1 + \frac{3(b+c)}{2b+c} \left(\frac{N_S}{N_T}\right)^{c-b} + \frac{3c}{b+2c} \left(\frac{N_S}{N_T}\right)^{2(c-b)}}{1 + 2 \left(\frac{N_S}{N_T}\right)^{(c-b)} + \left(\frac{N_S}{N_T}\right)^{2(c-b)}} \right] \quad (32)$$

$$S_{\text{axial}} = E\epsilon_T \left(\frac{N_S}{N_T}\right)^b \quad (33)$$

$$\frac{S_{\text{bending}}}{S_{\text{axial}}} = \text{correction factor} = \delta \quad (34)$$

$$\delta = \frac{1 + f_1 \left(\frac{N_S}{N_T}\right)^{(c-b)} + f_2 \left(\frac{N_S}{N_T}\right)^{2(c-b)}}{1 + 2 \left(\frac{N_S}{N_T}\right)^{(c-b)} + \left(\frac{N_S}{N_T}\right)^{2(c-b)}} \quad (35)$$

where

$$f_1 = \frac{3(b+c)}{2b+c} = \frac{1+n}{(2/3) + (1/3)n} \text{ where } n = c/b \quad (36)$$

$$f_2 = \frac{3c}{b+2c} = \frac{3n}{1+2n} \quad (37)$$

#### FLEXURAL BENDING OF CIRCULAR CROSS-SECTIONS

We calculate the bending moment required to produce a selected surface strain. From the selected surface strain fatigue life can be established and similarly nominal stresses from the required bending moment. Thus we establish the relation between nominal elastic stresses and fatigue life.

Figure 4 shows the notation used in the analysis. We assume a surface strain  $\epsilon_s$  corresponding to a life  $N_s$  when the full bending moment  $M$  is applied. Strain varies linearly across the section, so that the strain  $\epsilon_y$  at a distance  $y$  from the neutral axis is

$$\epsilon_y = \frac{y}{R} \epsilon_s$$

$$y = R \sin \theta, \quad dy = R \cos \theta d\theta \quad (38)$$

$$\epsilon_y = \epsilon_s \sin \theta \quad (39)$$

and the stress associated with the strain  $\epsilon_y$  can be found using Eq. (12),

$$\sigma_y = E \epsilon_T \left[ \left( \frac{\epsilon_s \sin \theta}{\epsilon_T} \right)^{z/b} + \left( \frac{\epsilon_s \sin \theta}{\epsilon_T} \right)^{z/c} \right]^{b/z} \quad (40)$$

where  $z$  is given by Eqs. (8) to (11).

The increment of bending moment contributed by a strip at the distance  $y$  from the neutral axis becomes

$$dM = y \cdot \sigma_y \cdot (\text{width of the strip}) \cdot dy$$

Substituting for  $y$  and  $dy$  from Eq. (38) and  $\sigma_y$  from Eq. (40),

$$dM = R \sin\theta \cdot E \epsilon_T \left[ \left( \frac{\epsilon_S \sin\theta}{\epsilon_T} \right)^{z/b} + \left( \frac{\epsilon_S \sin\theta}{\epsilon_T} \right)^{z/c} \right]^{z/b} 2R \cos\theta R \cos\theta d\theta \quad (41)$$

The total bending moment, taking into account the symmetrical contribution to bending moment of the section below the neutral axis is

$$M = 2 \int_{y=0}^{y=R} dM$$

$$M = 4R^3 E \epsilon_T \int_{\theta=0}^{\pi/2} \left[ \left( \frac{\epsilon_S \sin\theta}{\epsilon_T} \right)^{z/b} + \left( \frac{\epsilon_S \sin\theta}{\epsilon_T} \right)^{z/c} \right]^{z/b} \sin\theta \cos^2\theta d\theta \quad (42)$$

From Eq. (6),

$$\epsilon_S = \left( \frac{N_S}{N_T} \right)^b + \left( \frac{N_S}{N_T} \right)^c \quad (43)$$

where  $z$  is a function of  $(c/b)$  and  $(\epsilon_S/\epsilon_T)$  given by Eqs. (8)-(11).

It is clear from Eq. (42) that the integral does not lend itself to simple closed form solution. However, for any given material and a given surface strain, the integral can be computed numerically and the moment can be calculated. The nominal surface stress  $S_{\text{bending}}$  is expressed as:

$$S_{\text{bending}} = \frac{M R}{I} = \frac{M R 64}{\pi R^4} = \frac{64 M}{\pi R^3}$$

The ratio of nominal surface stress  $S$  to the stress that would be required to produce a life  $N_S$  in axial fatigue, can be written analogous to Eq. (35) by assuming the denominator and the exponent  $(c-b)$  remain the same for both rectangular and circular cross-sections.

$$\delta = \frac{1 + f_1 \left(\frac{N_S}{N_T}\right)^{(c-b)} + f_2 \left(\frac{N_S}{N_T}\right)^{2(c-b)}}{1 + 2 \left(\frac{N_S}{N_T}\right)^{(c-b)} + \left(\frac{N_S}{N_T}\right)^{2(c-b)}} \quad (44)$$

where  $f_1$  and  $f_2$  are for the circular cross-section. The ratio  $\delta$  is calculated numerically using Eqs. (43) and (42) for different values and combinations of parameters involved as follows:

$$\frac{N_S}{N_T} = 10^{-3}, 10^{-2}, \dots, 10^2, 10^3$$

$$c = -0.3, 0.4, \dots, -0.9, -1.0$$

$$b = -.05, -.06, \dots, -.19, -.20$$

Equation (44) can be written as

$$\delta \left[ 1 + 2 \left(\frac{N_S}{N_T}\right)^{(c-b)} + \left(\frac{N_S}{N_T}\right)^{2(c-b)} \right] = 1 + f_1 \left(\frac{N_S}{N_T}\right)^{(c-b)} + f_2 \left(\frac{N_S}{N_T}\right)^{2(c-b)} \quad (45a)$$

$$\left\{ \frac{\delta \left[ 1 + 2 \left(\frac{N_S}{N_T}\right)^{(c-b)} + \left(\frac{N_S}{N_T}\right)^{2(c-b)} \right] - 1}{\left(\frac{N_S}{N_T}\right)^{(c-b)}} \right\} = f_1 + f_2 \left(\frac{N_S}{N_T}\right)^{(c-b)} \quad (45b)$$



$$G\left(\frac{N_S}{N_T}, c, b, \delta\right) = f_1 + f_2 H\left(\frac{N_S}{N_T}, c, b\right) \quad (45)$$

If the function  $G$  is plotted against the function  $H$  for a given  $(c/b)$ , i.e.  $n$ , but for all combinations of  $c, b$ , and  $\frac{N_S}{N_T}$ , a straight line results. Thus the slope  $f_2$  and intercept  $f_1$  are functions of only  $n$ . The plot of  $G$  vs.  $H$  for different  $n$  values are shown in Fig. 5. For clarity the numerical values of functions  $G$  and  $H$  for different combinations of  $c, b$  and  $N_S/N_T$  are shown in Fig. 5 only for the case of  $n=5$ . The above procedure is repeated for several materials of various  $n$  values and the parameters  $f_1$  and  $f_2$  are calculated for each material with a specific  $n$ . They are shown in Fig. 6.

Since the parameters  $f_1$  and  $f_2$  are found to be functions of only  $n$ , an attempt was made to determine these functions whose form is analogous to ones shown for rectangular cross-section in Eqs. (36) and (37).

The functions were determined by least squares analysis to be

$$f_1 = \frac{1 + .8432 n}{.6849 + .255 n} \quad (46)$$

$$f_2 = \frac{2.6188 n}{1 + 1.5411 n} \quad (47)$$

The curves represented by the above functions are shown by solid lines in Figure 6.

For any given material the functions  $f_1$  and  $f_2$  can be calculated using the reciprocal of the strain hardening exponent,  $n$ , and Eqs. (46) and (47). The correction factor  $\delta$  and axial stress  $S_{axial}$  can be calculated for any given life using Eqs. (44) and (33), respectively. Thus we can plot nominal bending stress  $S_{bending}$  against life. The plots are shown in Fig. 7

for several materials of engineering interest. The properties of these materials, obtained from Ref. 7, are listed in Table II.

If the fatigue properties of the material are not known or cannot be obtained easily, Universal Slopes solutions can be used with the properties obtained from a tensile test. Universal plastic and elastic exponents of -0.6 and -0.12 are used, respectively. Transition strain  $\epsilon_T$  and transition life  $N_T$  can be determined from Eqs. (16) and (17), respectively.

#### DISCUSSION

The approach presented in this report takes into account only the effect of plastic flow in explaining the difference between axial and bending fatigue lives; hence, it is valid in the low cyclic life range. According to the analysis, the  $S_{axial}$  and  $S_{bending}$  curves become coincident for most engineering materials at lives greater than  $10^6$  cycles since the strains are purely elastic at those life levels and the  $M_c/I$  assumption is valid. However, bending fatigue life could still be higher than at axial fatigue for the same nominal stress due to volumetric effect which is not taken into account in the current approach. This is observed by Esin in steels and he has used micro-plastic strain energy criterion to take this factor into account (Ref. 8). This is also discussed in some detail in connection with risk-of-rupture criterion in Ref. 9. Basically, in bending fatigue lower volume of material is under high strain at outer fibers as compared to the whole volume in the axial case. Thus, the smaller the volume under maximum stress,

**ORIGINAL PAGE IS  
OF POOR QUALITY**

the lower will be the probability of the presence of a flaw at a point of high stress, hence the higher will be the life.

At high cyclic life range, the rotating bending will give lower life as compared to alternating bending for the same nominal stress which can be explained as follows. In alternating bending the regions A and B in Fig. 4 will be subjected to maximum surface strain, whereas in rotating bending all the material near the surface of the cylinder will be subjected to maximum strain at different times; for example, the region C will take the position of A or B while rotating, hence will be subjected to maximum strain. Thus, more volume is subjected to high stress in rotating bending hence greater will be the probability of the presence of a flaw at a point of high stress and lower will be the life.

It should be noted that results obtained in this report are valid for alternating flexural bending. If the material is subjected to rotating bending, the cross-section deflects about a different axis, which makes an angle with the loading axis ( Ref. 1). Once the angle between two axes is determined, the complete stress and strain distribution can be computed from which the bending moment for an assumed value of maximum surface strain can be established. In Ref. 1 it was observed that although the analysis for rotating bending is considerably more complicated than static flexural bending, the resulting strain distributions for the two cases differed little when considered in their respective bending planes. It was shown that the experimental results for rotating bending agreed well with the predictions made for static flexural bending. Hence it will be assumed here that the equations for flexural bending, Eq. (44) together with the  $f_1$  and  $f_2$  values given in Eqs. (46) and (47), are also valid for rotating bending in the low cycle fatigue range. Further study may be desirable to verify this assumption.

## CONCLUSION

Closed-form expressions were obtained for nominal bending stress in terms of axial fatigue stress based on true surface stresses. They are shown for rectangular and circular cross-sections in Table I. Using only axial fatigue data on a given material and formulas given in Table I, nominal bending stress-life curve can be established. Though the study is limited to only rectangular and circular cross-sections, the approach and the procedure described in this report can be applied to more complicated geometries to obtain the functional forms for parameters  $f_1$  and  $f_2$  which are functions of only strain hardening exponent of the material. The approach takes into account only the effect due to plastic flow which has dominating effect in the low cyclic life range. However, in the high cyclic life range other factors could be more dominating like the volumetric effect which should be taken into account in reconciling the difference between axial and bending fatigue lives. Future study is necessary to incorporate the volumetric effect in the analyses presented in this report.

ORIGINAL PAGE IS  
OF POOR QUALITY

REFERENCES

1. Manson, S.S., "Fatigue: A Complex Subject - Some Simple Approximations," Proceedings Society of Experimental Stress Analysis 12, No. 2 (1965).
2. Manson, S.S., "Thermal Stress in Design, Part 19, Cyclic Life of Ductile Materials," Machine Design (July 7, 1960), pp. 139-144.
3. Morrow, J., "Cyclic Plastic Strain Energy and Fatigue of Metals," ASTM STP 378 (1965), pp. 45-87.
4. Smith, R.W., Hirschberg, M.H., and Manson, S.S., "Fatigue Behavior of Materials Under Strain Cycling in Low and Intermediate Life Range," NASA-TN-D-1574, April 1963.
5. Manson, S.S., "Predictive Analysis of Metal Fatigue in the High Cycle Life Range," Methods for Predicting Material Life in Fatigue, The Winter Annual Meeting of the ASME Dec. 2-7, 1979, pp. 145-183.
6. Manson, S.S. and U. Muralidharan, "A Single Expression Formula for Inverting Strain-Life and Stress-Strain Relationships," NASA CR-165347.
7. Landgraf, R.N., Mitchell, M.R. and LaPointe, N.R., "Monotonic and Cyclic Properties of Engineering Materials," Ford Motor Company (1972).
8. Esin, A., "A method for correlating different types of fatigue curve," International Journal of Fatigue, Vol. 2, No. 4, Oct. 1980, pp. 153-158.
9. Manson, S.S., "Thermal Stress and Low-cycle Fatigue," Robert E. Kreiger Publishing Company, Malabar, Florida, 198 , sec. 7.1.7 and 7.1.8.

TABLE I

$n = c/b$  ratio of plastic to elastic exponents

$$\epsilon_T = \text{transition strain range} = 2\epsilon_f' \cdot 1^{-n} \left( \frac{\sigma_f'}{E} \right)^{\frac{n}{n-1}}$$

where  $\epsilon_f'$  = fatigue ductility coefficient

$\sigma_f'$  = fatigue strength coefficient

$E$  = modulus of elasticity

$$N_T = \text{Transition life} = \frac{1}{2} \left( \frac{E\epsilon_f'}{\sigma_f'} \right)^{\frac{1}{b-c}}$$

$$\epsilon_{\text{axial}} = E\epsilon_T \left( \frac{N_S}{N_T} \right)^b$$

$$S_{\text{bending}} = \left[ \frac{1 + f_1 \left( \frac{N_S}{N_T} \right)^{(c-b)} + f_2 \left( \frac{N_S}{N_T} \right)^{2(c-b)}}{1 + 2 \left( \frac{N_S}{N_T} \right)^{(c-b)} + \left( \frac{N_S}{N_T} \right)^{2(c-b)}} \right] S_{\text{axial}}$$

where  $f_1$  and  $f_2$  are functions of  $n$  and depend on the geometry of the cross-section.

For Rectangular Section

$$f_1 = \frac{1+n}{(2/3) + (1/3)n}$$

$$f_2 = \frac{3n}{1+2n}$$

For Circular Cross-section

$$f_1 = \frac{1 + .8432 n}{.6849 + .255 n}$$

$$f_2 = \frac{2.6188 n}{1 + 1.5411 n}$$

For any given surface strain  $\epsilon_s$ , surface life  $N_s$  can be found from Fig. 2 and  $S_{\text{axial}}$  and  $S_{\text{bending}}$  can be computed using the above formulas.

Table II

1 MATERIAL	2 σ <sub>u</sub> ksi	3 ε <sub>f</sub>	4 b	5 C	6 E ksi	7 S <sub>T</sub>	8 N <sub>T</sub> Cycles
01 SAE1005-1009 NRLC	70	.11	-.073	-.41	29000	2.41E10	30300
02 GAINEX (NRLC)	117	.06	-.071	-.65	29200	4.15E10	5322
03 MAH-TED-150BMM	141	.05	-.11	-.59	30000	2.06E10	252.9
04 SAE1045-225 BMM	178	1.0	-.095	-.66	29000	5.21E10	4114
05 SAE1045-390 BMM	230	.45	-.074	-.68	30000	9.35E10	414
06 SAE1045-410 BMM	270	.60	-.073	-.70	29000	.01166	384
07 SAE1045-450 BMM	260	.35	-.07	-.69	30000	.01142	195
08 SAE1045-595 BMM	395	.07	-.081	-.60	30000	.0203	12.5
09 10862-430 BMM	258	.32	-.067	-.56	28000	.0114	667
010 AISI4130-365 BMM	246	.09	-.081	-.69	29000	9.14E10	1041
011 SAE4142-475 BMM	315	.09	-.081	-.61	30000	.01511	29
012 SAE4142-560 BMM	385	.07	-.089	-.76	30000	.0205	6.27
013 T1-6AL-4V	552.4	1.053	-.1052	-.6903	17000	.0348	191
014 SAE4142-400 BMM	275	.5	-.09	-.75	29000	.011	203.3
015 SAE4142-450 BMM	290	.60	-.08	-.73	30000	.0122	154
016 SAE4142-475 BMM	300	.20	-.082	-.77	29000	.0145	37
017 AISI4340-243 BMM	174	.45	-.095	-.54	28000	4.90E10	7557
018 AISI4340-409 BMM	290	.68	-.091	-.60	29000	.01	1005
019 SAE5160-430 BMM	280	.60	-.071	-.57	28000	.0118	812
020 SAE9262-260 BMM	151	.155	-.071	-.47	30000	5.47E10	2688
021 SAE9262-410 BMM	269	.38	-.057	-.65	29000	.013	262
022 AISI304-160 BMM	350	1.02	-.15	-.77	27000	9.02E10	571.3
023 AISI316-145 BMM	260	.60	-.15	-.57	28000	3.76E10	12761
024 A1350 Annealed	406	.33	-.14	-.84	28000	.016	63.4
025 182 H1-Straging 440 BMM	310	.80	-.071	-.79	27000	.015	183

Table II (Continued)

1 MATERIAL	2 $\sigma_p$ ksi	3 $\sigma_f$	4 b	5 c	6 E ksi	7 $A_{cT}$	8 $N_T$ Cycles
#26 18X Nickel Manganese 400 BHN	325	.60	-.07	-.75	26000	.017	648
#30 2014-Al-76	123	.42	-.106	-.65	10000	.0124	329
#31 2014-Al-74	167	.21	-.11	-.52	10200	.0140	344
#32 5456 Aluminum	105	.46	-.11	-.67	10000	9.99X10 <sup>-3</sup>	427
#33 SAE1015-80 BHN	120	.95	-.11	-.64	30000	2.57X10 <sup>-3</sup>	15183
#34 SAE9501-150 BHN	91	.35	-.075	-.54	30000	2.82X10 <sup>-3</sup>	13604
#35 VAMCO-225 BHN	153	.21	-.08	-.53	28200	5.67X10 <sup>-3</sup>	1688
#36 RQC100-298 BHN	167	.60	-.076	-.57	29400	5.42X10 <sup>-3</sup>	1582
#37 SAE1045-500 BHN	330	.25	-.08	-.68	30000	.0145	91
#38 AISI4130-258 BHN	185	.92	-.083	-.63	32000	5.36X10 <sup>-3</sup>	5298
#39 SAE4142-380 BHN	265	.45	-.08	-.75	30000	.0110	177
#40 SAE4142-450 BHN	305	.60	-.09	-.76	29000	.0122	209
#41 SAE4340-350 BHN	240	.73	-.076	-.62	28000	9.21X10 <sup>-3</sup>	1767
#42 AISI52100-518 BHN	375	.18	-.09	-.56	30000	.015	146
#43 SAE9267-280 BHN	177	.41	-.073	-.60	28000	7.09X10 <sup>-3</sup>	1372
#44 B-11 660 BHN	660	.08	-.077	-.74	30000	.0253	6
#45 AISI304-327 BHN	330	.89	-.12	-.69	25000	.0109	808
#46 AM350-496 BHN	390	.098	-.102	-.42	26000	.0164	183
#47 18X Nickel Manganese 450 BHN	240	.3	-.065	-.62	27000	.0118	284
#48 2024-T351 Aluminum	160	.22	-.124	-.59	10600	.0148	157
#49 7075-T6 Aluminum	191	.19	-.126	-.52	10300	.0176	184
#50 SAE1005-NRLC	93	.1	-.154	-.39	29000	1.69X10 <sup>-3</sup>	103608



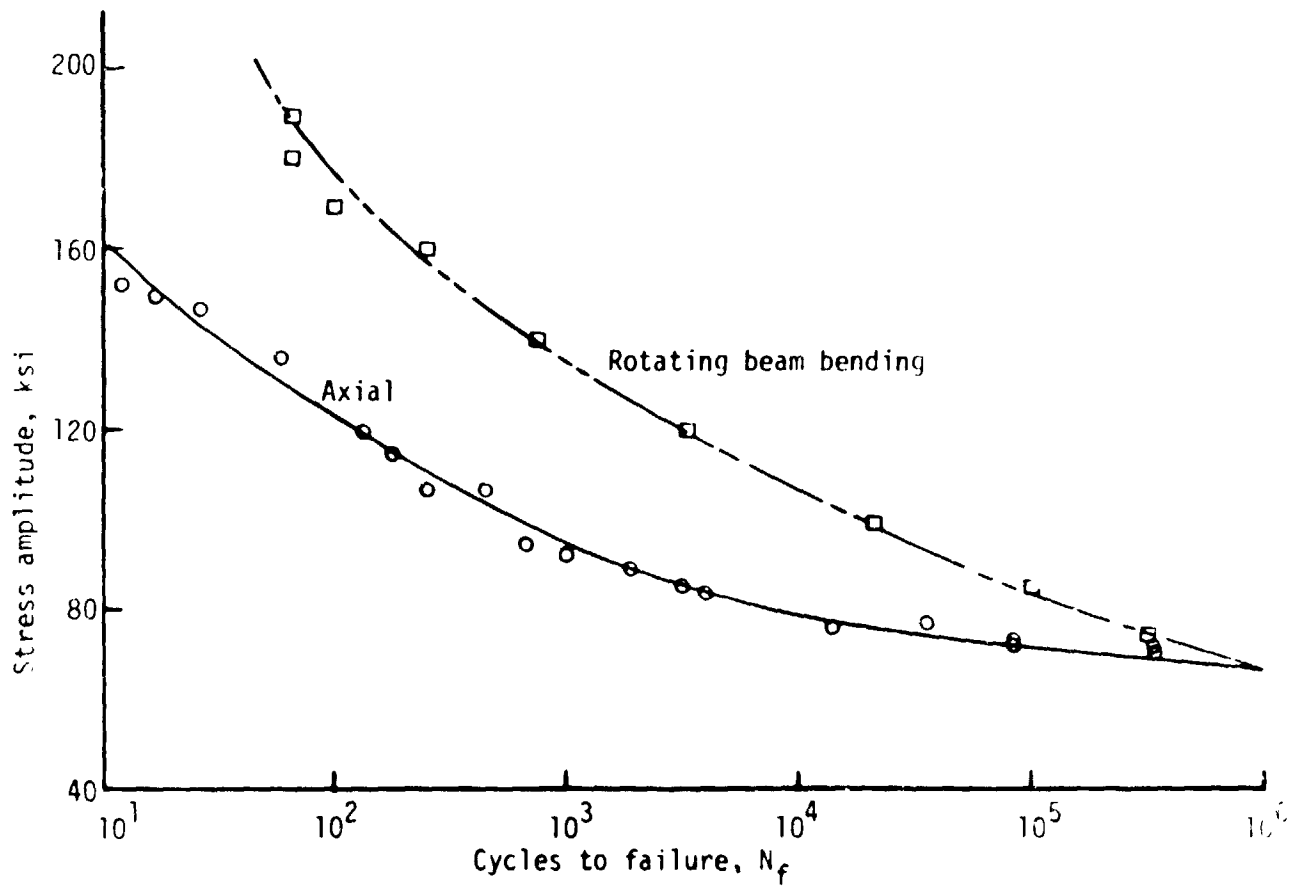


Fig. 1. Fatigue data under axial loading and in rotating bending for 4130 steel from Ref. 1.

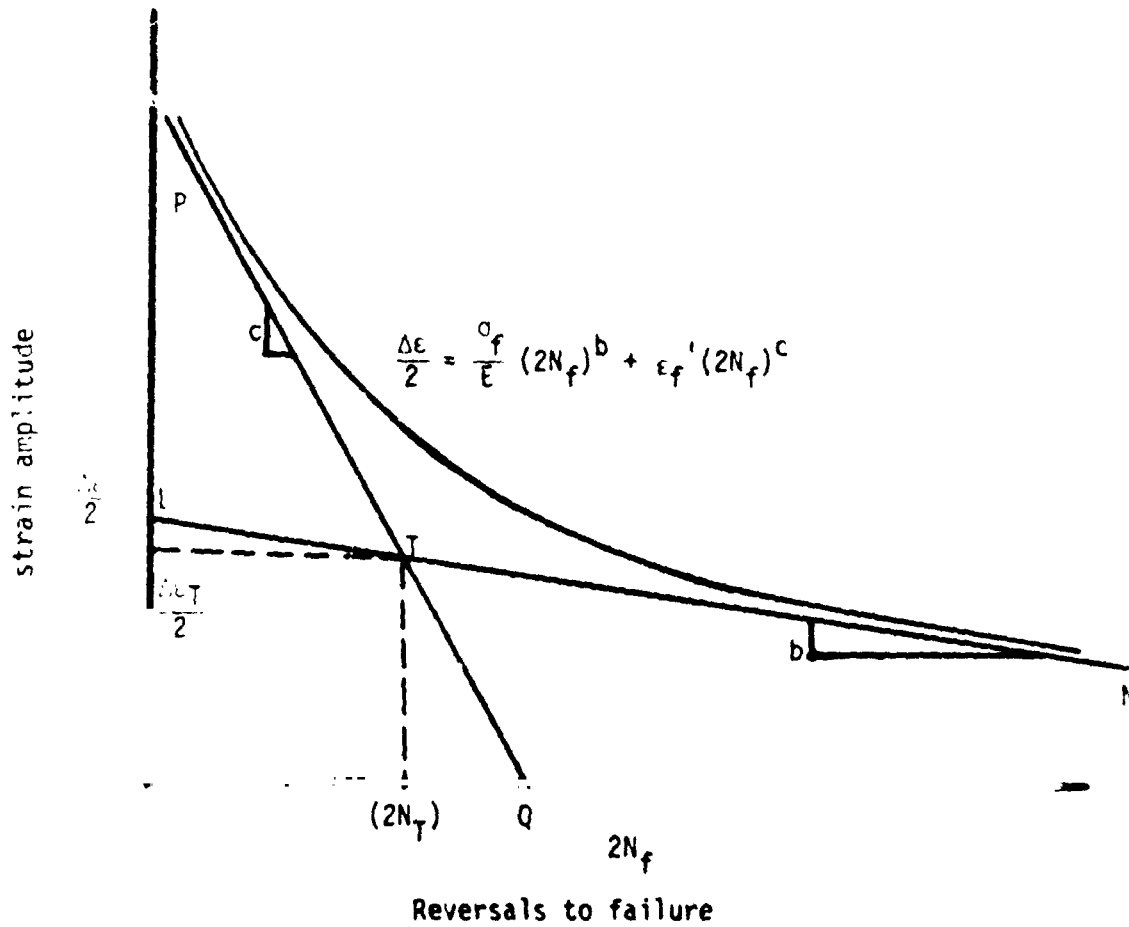


Fig. 2. Model of fatigue life relationship consisting of linear elastic and plastic components on double logarithmic coordinates.

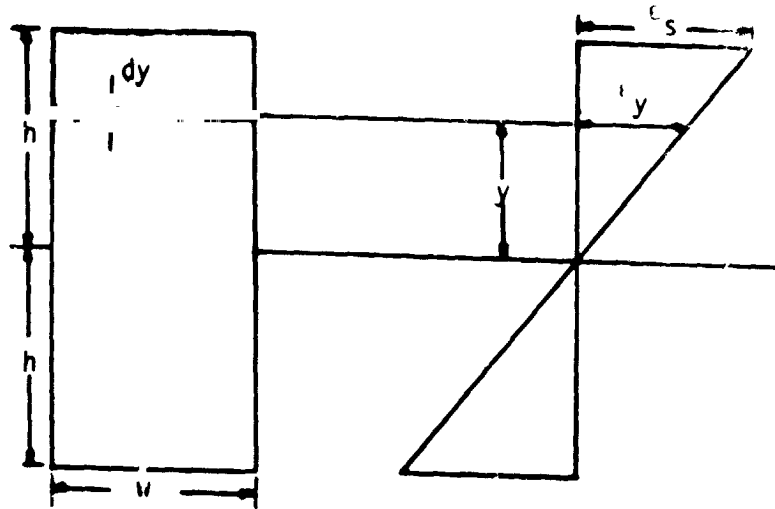


Fig. 3. Rectangular cross-sectional bar in flexural bending.

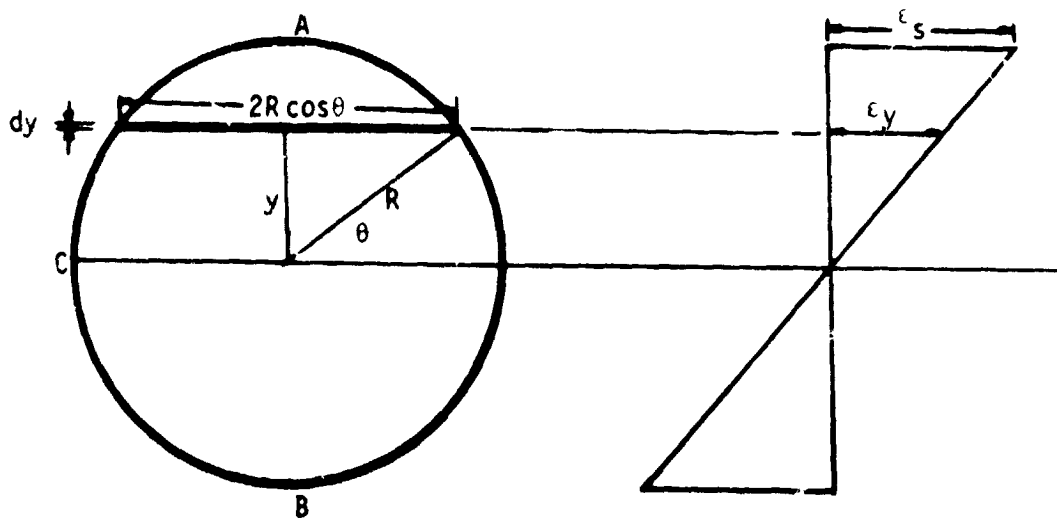


Fig. 4. Circular cross-sectional bar in flexural bending.

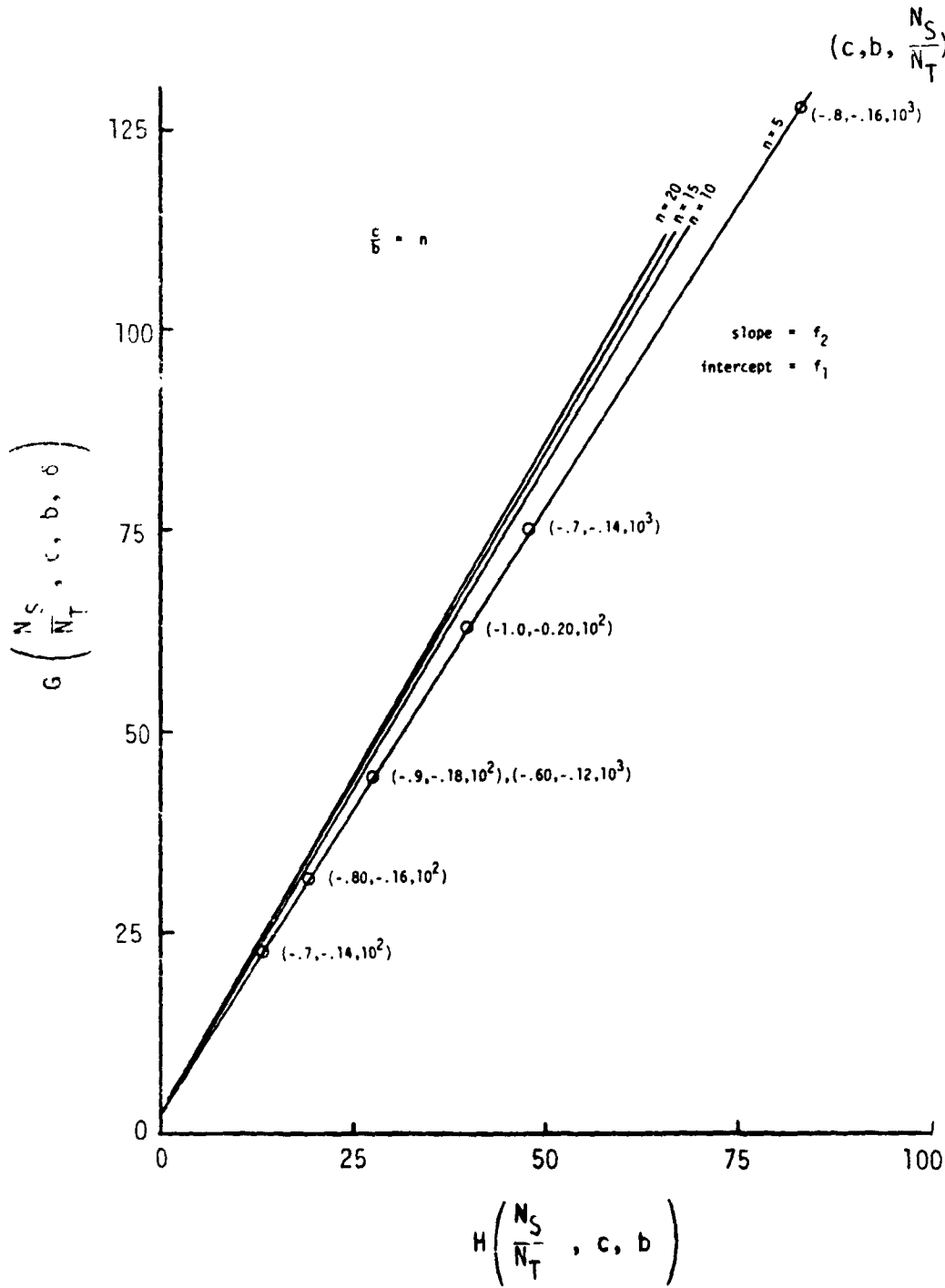


Fig. 5. Plot of G vs. H for a given  $c/b$  and for all combinations of  $c, b$  and  $(N_S/N_T)$  showing  $f_1$  and  $f_2$  are functions of only  $(c/b)$ .

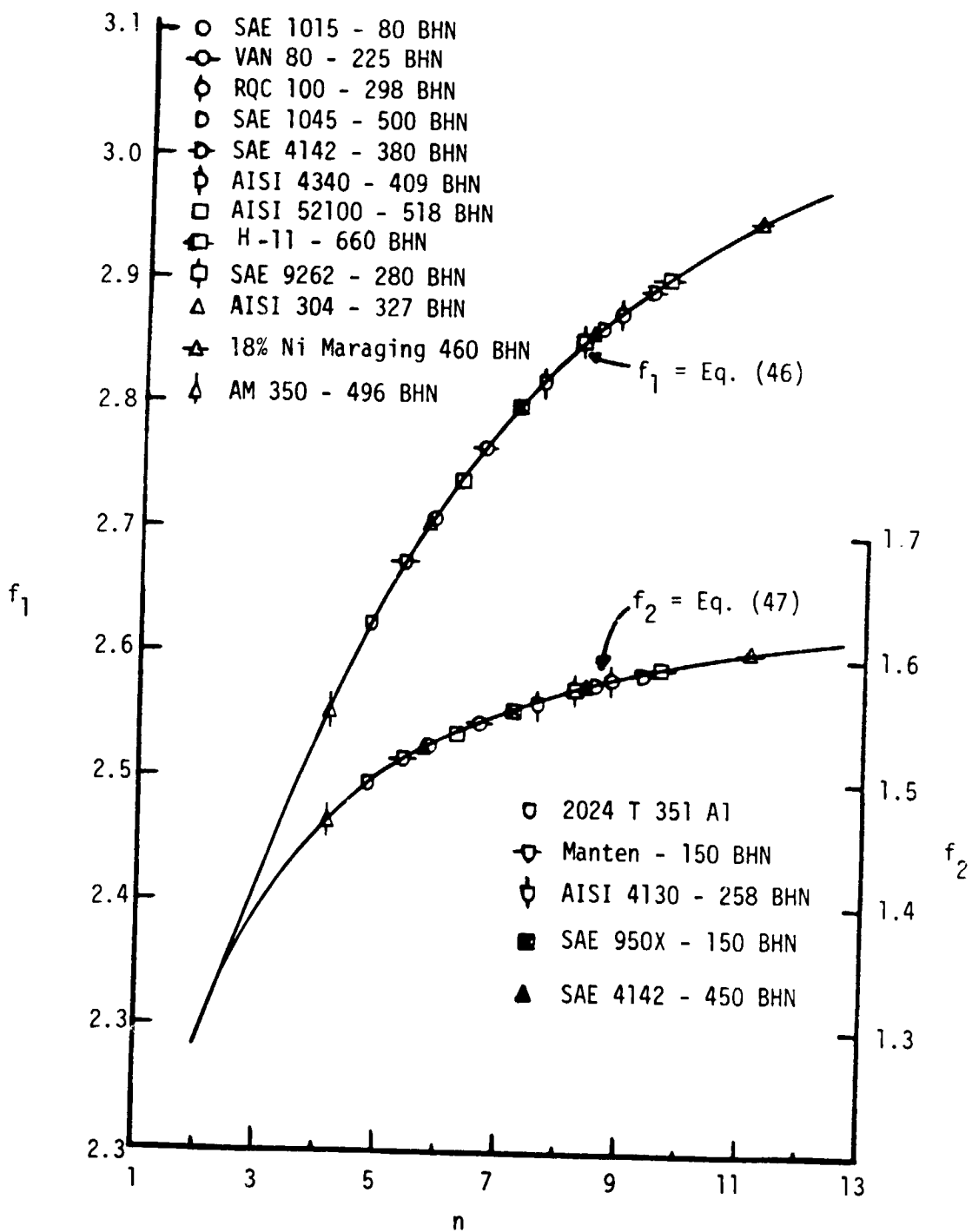


Fig. 6. The parameters  $f_1$  and  $f_2$  are shown for materials with different  $n$  values. The solid lines are curve-fits given by Eqs. (46) and (47), respectively.

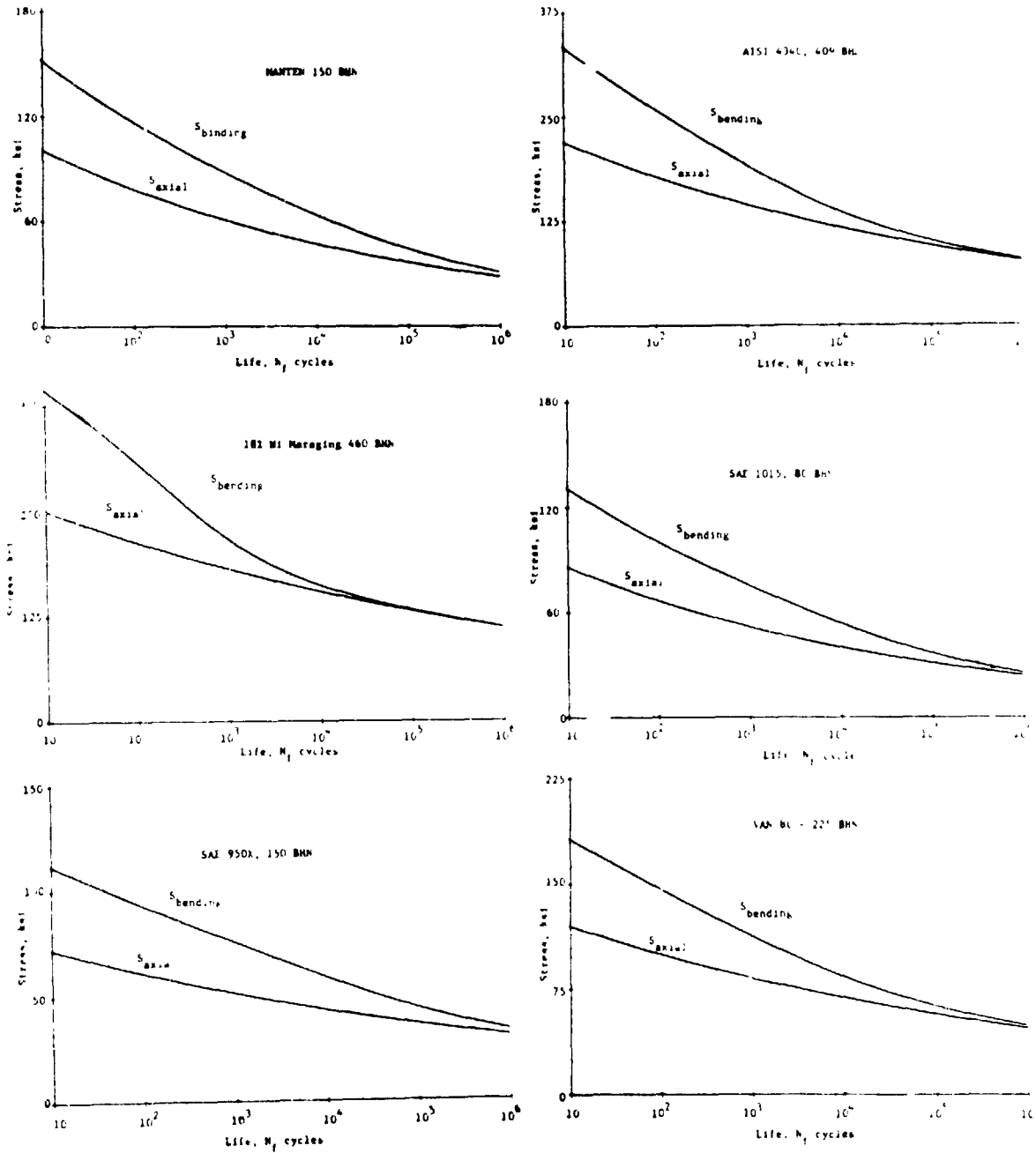


Fig. 7. Axial stress and nominal bending stress are plotted against life for various materials using formulas summarized in Table I.

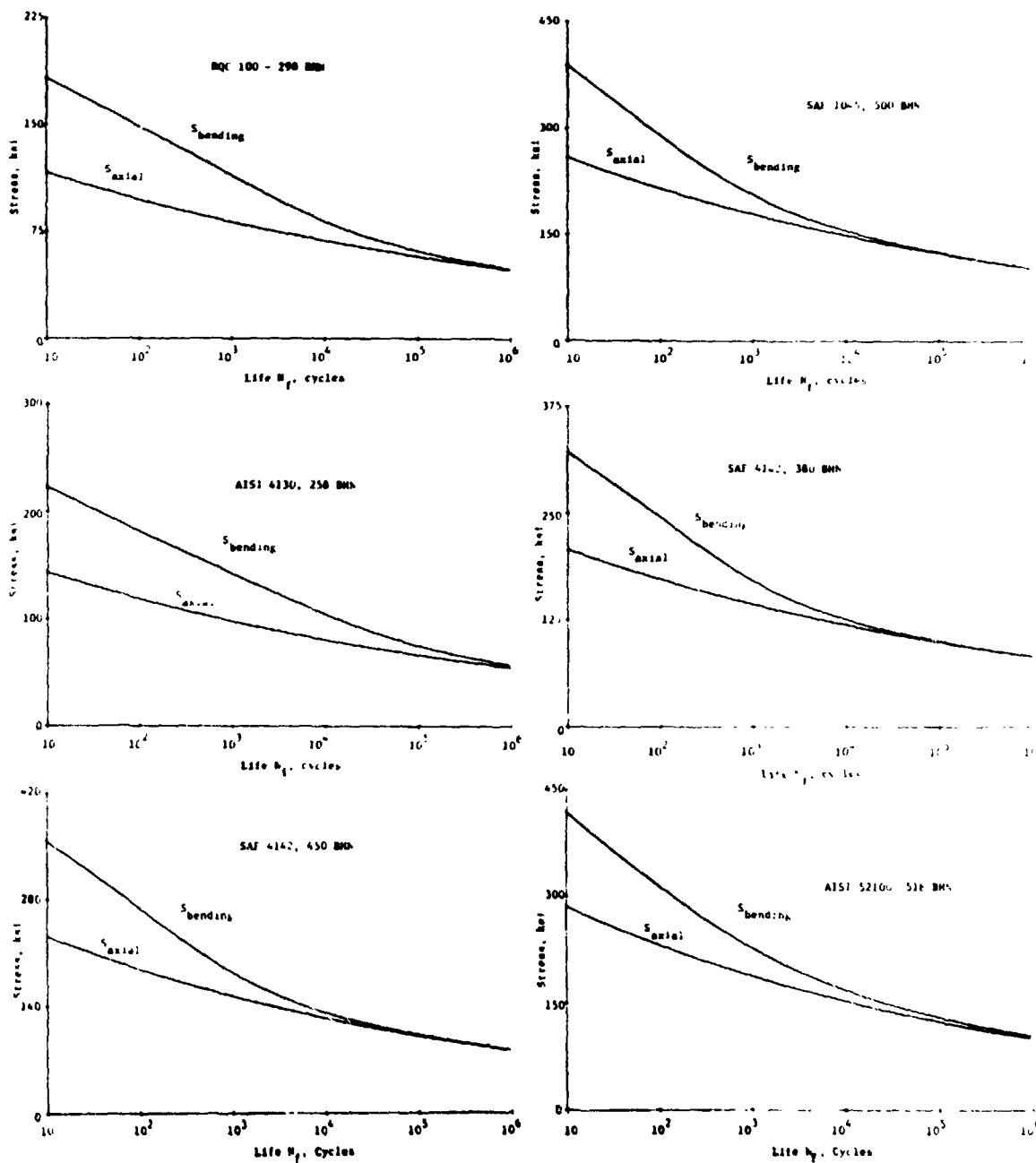


Fig. 7 (Continued)

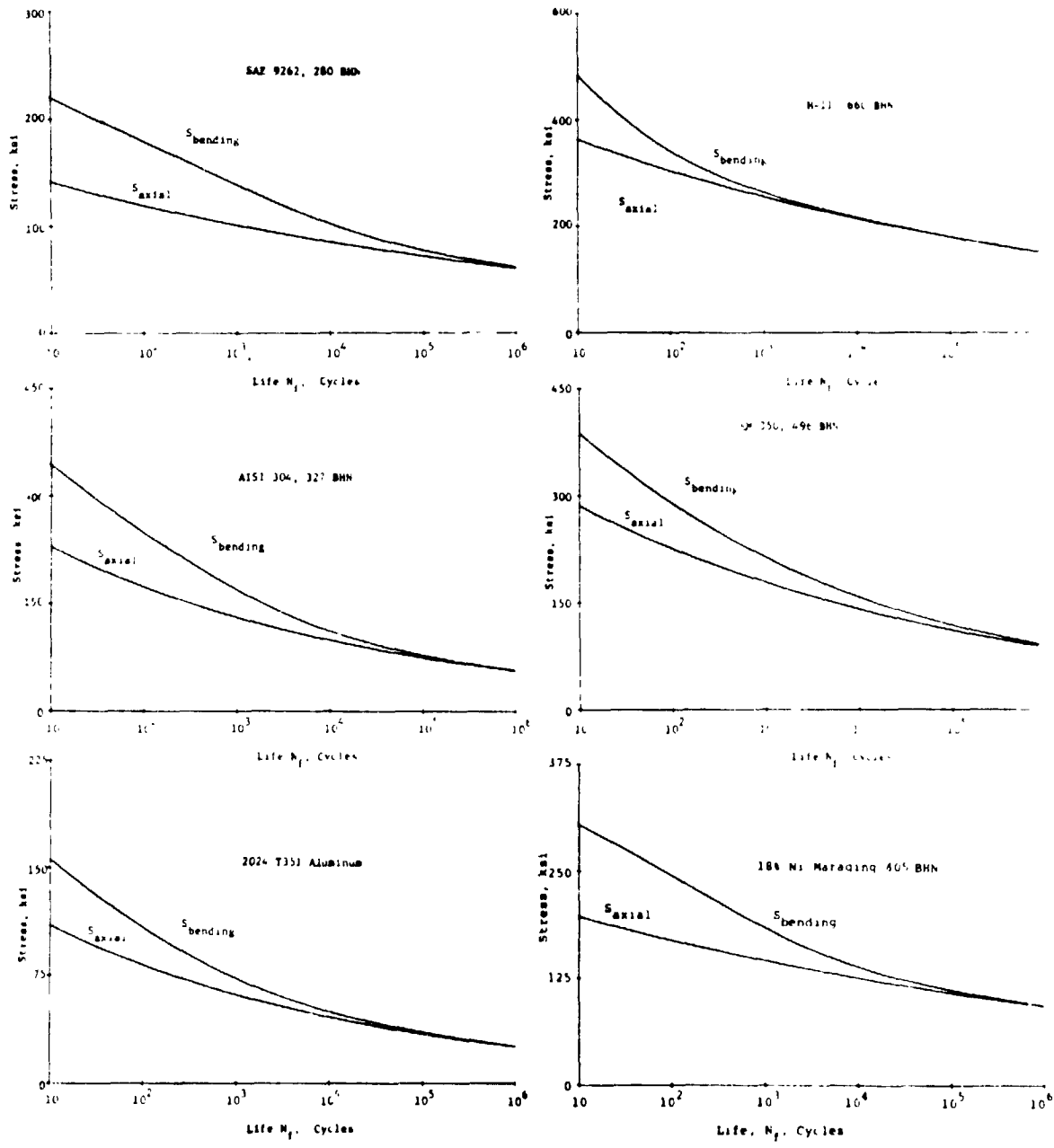


Fig. 7 (Continued)



ORIGINAL

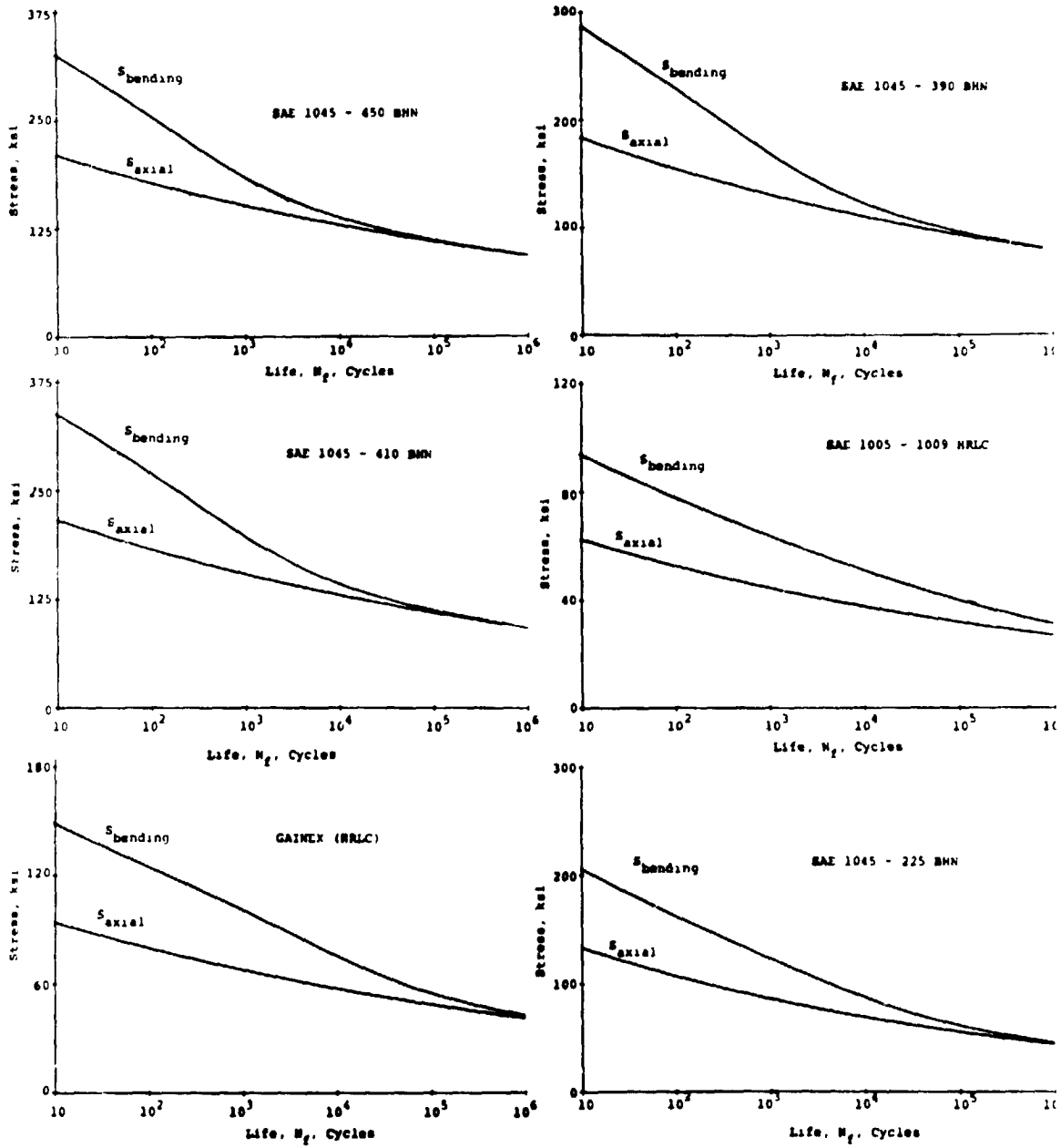


Fig. 7 (Continued)

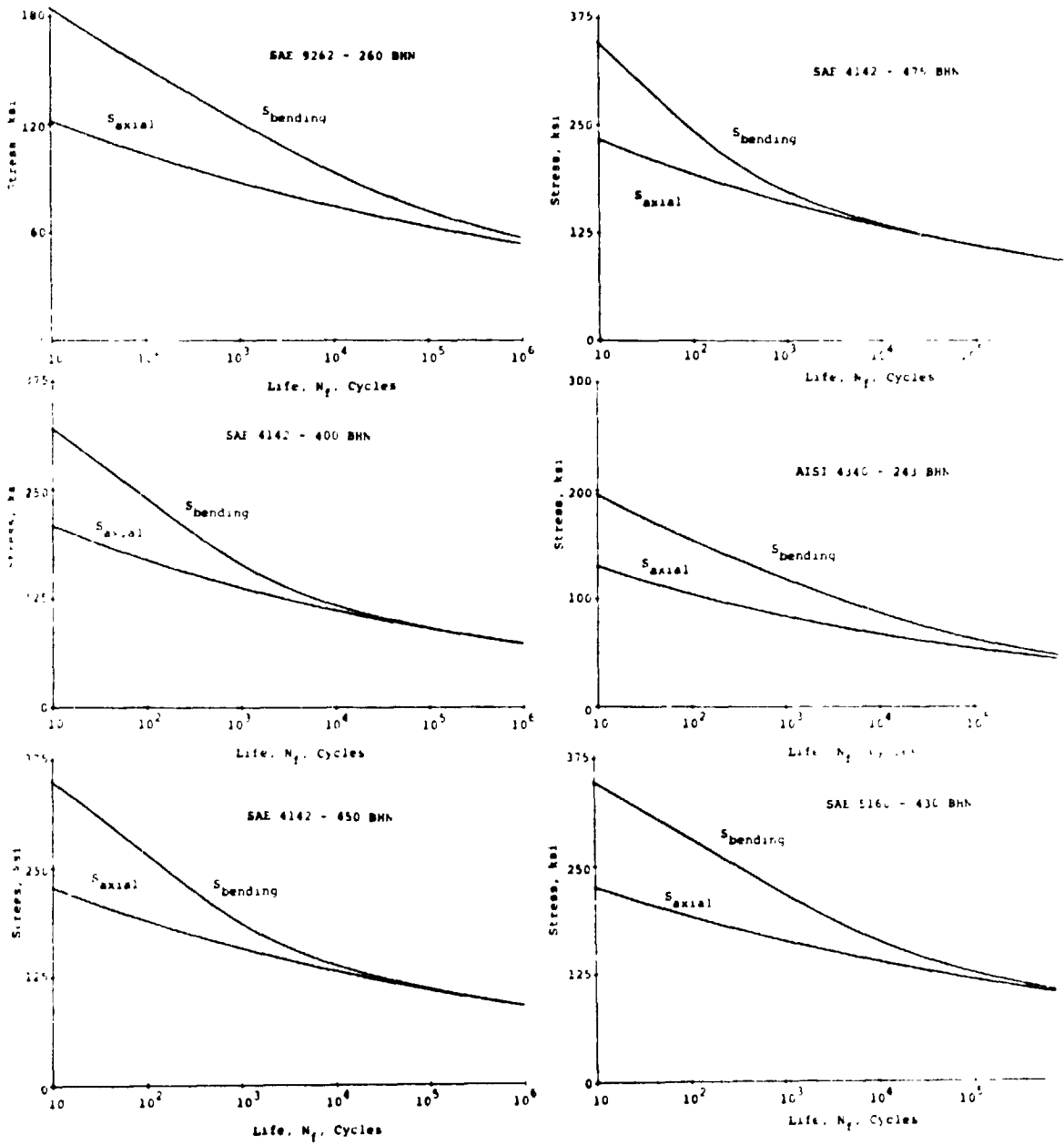


Fig. 7 (Continued)

ORIGINAL PAGE IS  
OF POOR QUALITY

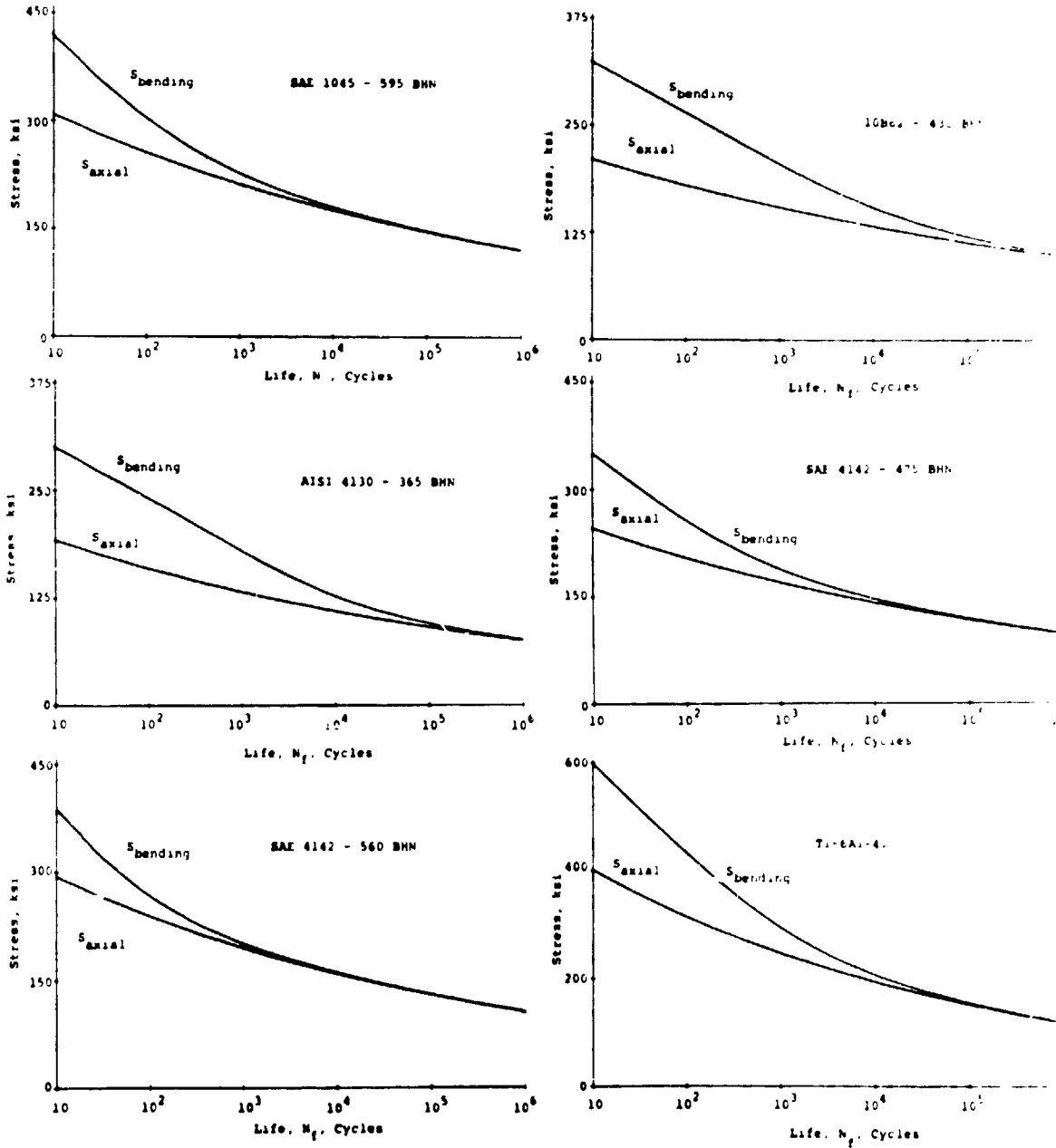


Fig. 7 (Continued)

ORIGINAL PART IS  
OF POOR QUALITY

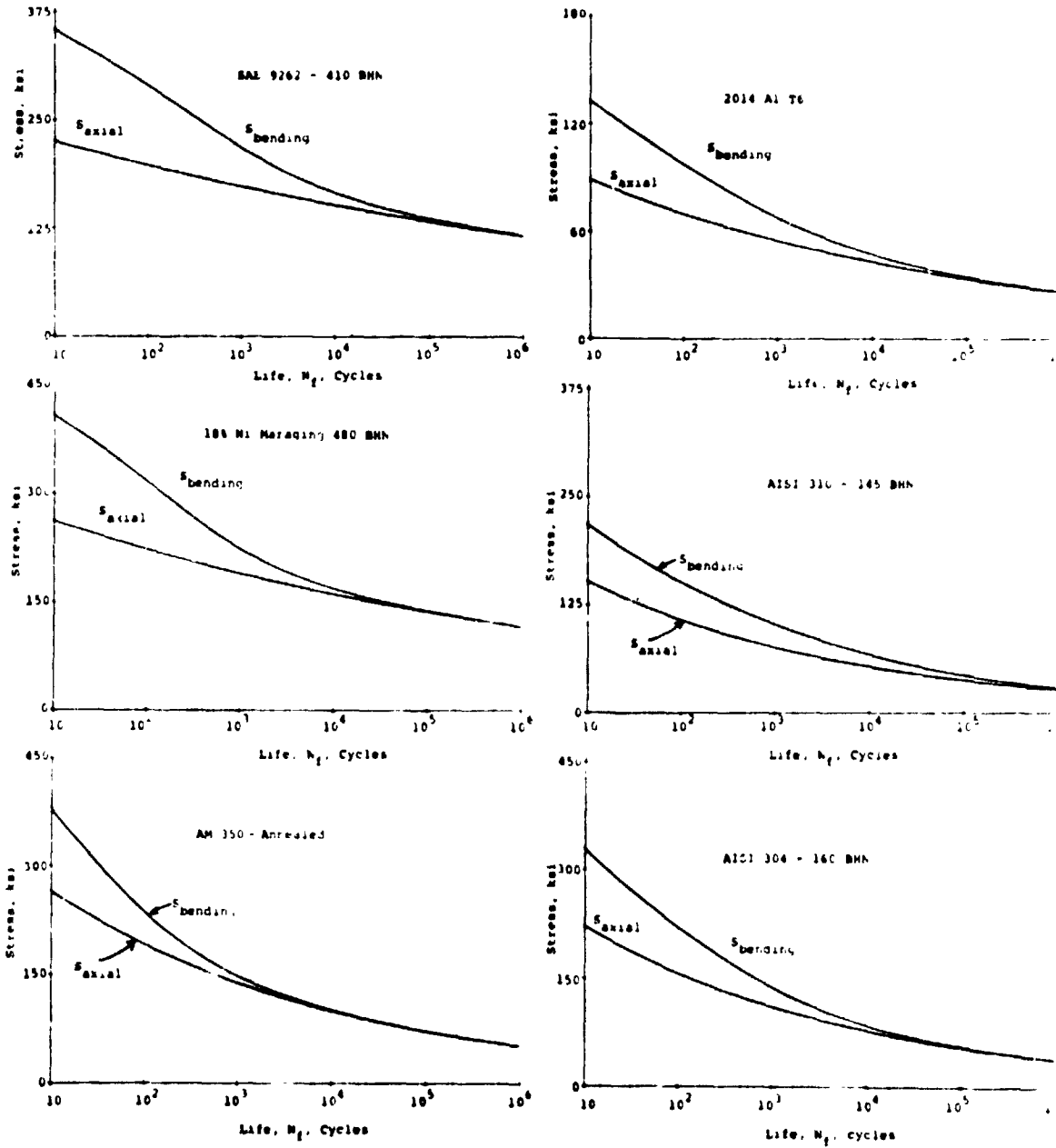


Fig. 7 (Continued)

ORIGINAL PAGE IS  
OF POOR QUALITY

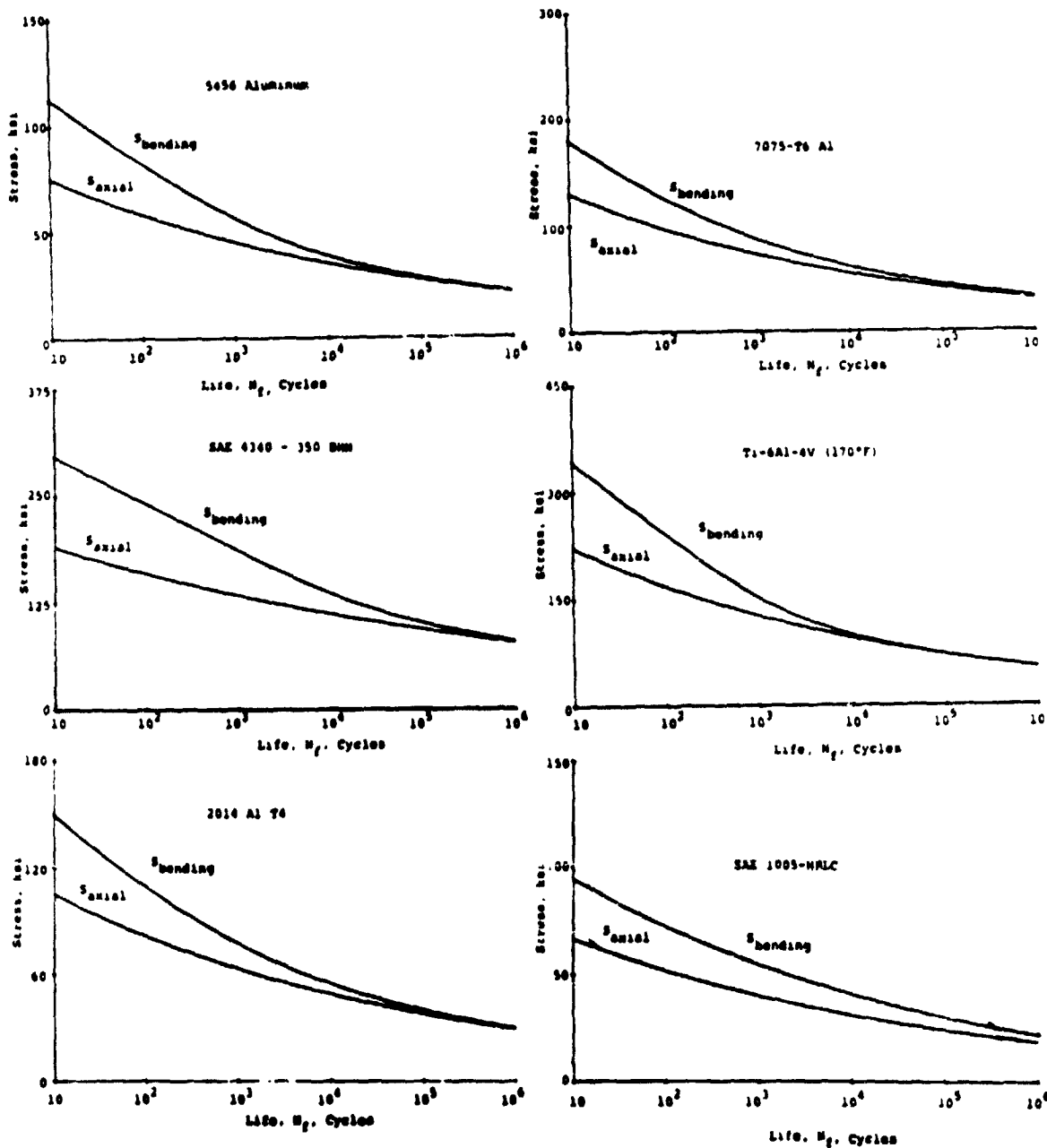


Fig. 7 (Continued)